

## Miscibility and rheologically determined phase diagram of poly(ethylene oxide)/poly( $\epsilon$ -caprolactone) blends

Jingqing Li · Yao Zhang · Yundan Jiacao ·  
Yingrui Shang · Hong Huo · Shichun Jiang

Received: 10 August 2011 / Revised: 12 November 2011 / Accepted: 27 November 2011 /  
Published online: 3 December 2011  
© Springer-Verlag 2011

**Abstract** Poly(ethylene oxide)/poly( $\epsilon$ -caprolactone) (PEO/PCL) blends can be widely used in lithium rechargeable battery area or as medical materials, while the miscibility and phase diagram of the blends are still unclear. The present work attempted to establish the blends' phase diagram using rheometry and investigated the miscibility. The results showed that a miscibility window of upper critical solution temperature character of the blends is revealed. Meanwhile, the abnormal rheological behavior of PEO at temperatures higher than 130 °C has little influence on the phase diagram determination. Different rheological properties of PEO/PCL blends from those of PEO revealed the existence of interactions between PEO and PCL molecular chains. Whereas shear-induced mixing or shear-induced phase separation might occur in phase diagram determination of PEO/PCL blends using rheometry.

**Keywords** Poly(ethylene oxide) · Poly( $\epsilon$ -caprolactone) · Polymer blends · Rheology · Phase diagram

---

J. Li (✉) · Y. Zhang · Y. Jiacao · Y. Shang · S. Jiang (✉)  
Tianjin Key Laboratory of Composite and Functional Materials, School of Materials Science and Engineering, Tianjin University, Tianjin 300072, People's Republic of China  
e-mail: jqli11103@tju.edu.cn

S. Jiang  
e-mail: scjiang@tju.edu.cn

H. Huo  
Institute of Polymer Chemistry and Physics, College of Chemistry, Beijing Normal University,  
Beijing 100875, People's Republic of China

## Introduction

In the past decades, polymer blends, miscible or immiscible, were believed to have some superior functional and mechanical properties than homopolymers. Due to their promising technological applications and the related scientific problems, polymer blends had attracted many researchers' interests [1–11]. As known, the properties of a miscible polymer blend are mainly attributed to its composition and the molecular interaction between the chains of different components [2, 3]. The properties of an immiscible polymer blend are closely related to its phase structure and the properties of its components [4–8]. Comparing with a miscible polymer blend, an immiscible blend usually shows a complex dependence of its properties on its additional phase structure. Therefore, it can be deduced that the miscibility of a polymer blend greatly affects its properties and applications. Many research groups [2, 3, 9–16] have been devoted to investigating on the miscibility of different polymer blends and their phase diagram establishment in favor of their promising technological applications in industry.

Of course, the properties of the polymer blends can be used to assess the miscibility of the mixture [12, 13]. That is, in miscible polymer blends, the components are well mixed on molecular level with no aggregations of components. Once the aggregations emerge in polymer blends, the blends are immiscible and always show additional elasticity due to the formed interfaces [8, 12, 13]. Many experimental methods have been developed to measure the miscibility of the blends and then help to establish the phase diagram of the mixture [9–13]. For example, differential scanning calorimetry (DSC), dynamic mechanical analysis (DMA), small angle X-ray scattering (SAXS), small angle light scattering (SALS), phase contrast microscopy (PCM), and rheometry are all efficient tools to investigate the miscibility of polymer blends and then to establish their phase diagrams. Though in practice, for a certain polymer blend system, only some of the above experimental methods are suitable.

Poly(ethylene oxide)/poly( $\epsilon$ -caprolactone) (PEO/PCL) blend can be developed as a promising polymer material in lithium rechargeable batteries [17–22]. It is also widely used in controlled drug delivery [23–25], drug-loaded biodegradable nerve guides [26], and porous scaffolds for tissue engineering [27]. All these applications of PEO/PCL blends are mainly based on the characteristic properties of PEO or PCL components, compositions, and corresponding phase structures of the blends. In applications such as PEO-based electrolytes or PCL-based medical materials, the properties of PEO/PCL blends should be tunable by tailoring its composition and phase structure while blending. So, it is important to estimate the miscibility and establish the phase diagram of PEO/PCL blends. Many researchers [9–11, 28, 29] have tried different experimental methods to work on this subject in recent years. However, for PEO/PCL blends, some of the used experimental methods are not efficient in this purpose. Different researchers even drew contradictory conclusions from their observations.

By measuring the changes of glass transition temperatures ( $T_g$ ) of components in polymer blends, DSC and DMA have been developed as important tools to investigate the miscibility of polymer blends. However, the  $T_g$  values of PEO and

PCL are so close to each other that DSC or DMA cannot recognize the separated  $T_g$ s of the components. Of course, their shifts in such a polymer blend are thus difficult to be detected. One obtained apparent single peak in a blend may be just the physical summary of the two peaks of the components without any obvious indications of increasing or decreasing miscibility of polymer blends. For example, Kuo et al. [9] had reported that both PEO ( $M_{n,PEO} = 20,000$  g/mol) and PCL materials ( $M_{n,PCL} = 80,300$  g/mol) they used have the same  $T_g$  values of  $-60$  °C. This makes it impossible to determine the miscibility of PEO/PCL blends by using one or two  $T_g$  values of the components in the blends with different compositions. To the authors' knowledge, no results have been reported to determine the miscibility of PEO/PCL by variations of  $T_g$  values of PEO and PCL, which indicated that DSC or DMA methods are not suitable to investigate the miscibility of PEO/PCL blends. Similarly, the electronic density of PEO is also very close to that of PCL and SAXS cannot be used to determine the miscibility of PEO/PCL, too.

By time-resolved SALS (TRSALS), Chuang et al. [11] reported their investigations on the kinetics of liquid–liquid phase separation for the blends of poly(ethylene glycol) (PEG)/PCL. It is known that PEG has the same molecular structure unit as in PEO, only with much smaller molecular mass. When liquid–liquid phase separation is reached in PEG/PCL blend, the transmitted light intensity shows a sudden decrease with decreasing temperature. The authors defined the onset temperatures of the light intensity as the phase-separation temperatures of the PEG/PCL blends. The whole binodal line is thus determined by cloud-point method. After the time evolution of scattering, profile is analyzed by linear Cahn–Hilliard theory for early stage of spinodal decomposition, the spinodal line is also drawn. The results showed PEG/PCL blends reveal a miscibility window of upper critical solution temperature (UCST) character. By PCM, Qiu et al. [10] examined the miscibility of PEO/PCL blends and they observed clearly defined biphasic separation of PEO/PCL blends at  $90$  °C with varying PEO content in the mixture, indicating that PEO is not miscible with PCL in the melt. The results of PCM observations of Qiu et al. agree with the UCST-type phase diagram determined by Chuang et al., and it can be concluded that PEO and PCL are immiscible in their amorphous phases at room temperature, though the polymers used in different works by Chuang et al. ( $M_{w,PEG} = 400$  g/mol and  $M_{w,PCL} = 10,000$  g/mol) and Qiu et al. ( $M_{w,PEO} = 100,000$  g/mol and  $M_{w,PCL} = 14,300$  g/mol) are of different molecular mass.

However, Kuo et al. [9] found that the crystallization temperatures ( $T_c$ ) of PEO/PCL blend, determined by DSC, are depressed with their respective homopolymers. This result reveals that the PEO or PCL chains are able to penetrate and to insert into the lamella region of other homopolymers. Furthermore, Kuo et al. [9] designed a ternary polymer blend of phenolic resin, PEO, and PCL and investigated the phase behavior and hydrogen bonding in this system using DSC and Fourier transform infrared spectroscopy (FTIR). Then, they indirectly determined the interaction energy density value of PEO/PCL as  $-2.85$  cal/cm<sup>3</sup> by comparing the experimental data of the ternary phenolic/PEO/PCL blends with the theoretically predicted spinodal phase diagram based on the Flory–Huggins lattice model. They concluded

that this negative value of  $B_{\text{PEO/PCL}}$  agreed well with the  $T_c$  depression of PEO/PCL blends and both of them indicated that PEO/PCL is miscible in the amorphous phase at room temperature.

As noticed, Kuo et al. used indirect experimental methods to investigate the miscibility of PEO/PCL blends; their conclusions are contradictory to the aforementioned SALS experiments of Chuang et al. and PCM observations of Qiu et al. The miscibility and phase diagram of PEO/PCL blends are still questionable. The agreement and disagreement of experimental observations indicated that further investigations are demanded to confirm the miscibility and phase diagram of the PEO/PCL blends. The present work is an attempt to determine the miscibility and to establish the phase diagram of PEO/PCL blends using a method of dynamic shear rheology, which has been proved to be a powerful experimental method for many other polymer blends previously [12–14, 34].

## Experimental

### Materials

The PEO and PCL materials were obtained from Polysciences. The weight-average molecular weights ( $M_w$ ) are of 20,000 and 20,000 g/mol for PEO and PCL, respectively. And the  $M_w/M_n$  ratios for PEO and PCL are of 1.1 and 2.08, respectively.

### Sample preparation

The PEO/PCL blends were prepared by solution blending with tetrahydrofuran (THF) as solvent. The weight proportions of the blends were 90/10, 80/20, 70/30, 60/40, 50/50, 40/60, 30/70, 20/80, and 10/90. After PEO and PCL were solved completely in THF, the solvent was evaporated mostly at 40 °C. Then, the samples were dried at 40 °C for a week and then moved into a vacuum chamber at 40 °C for another week in order to remove the solvent remnants of the preparation method. During the drying process of these samples, their weights were also checked carefully to be constants. The obtained powders of the blends were then molded into sample disks at room temperature with thickness of 0.6 mm and diameter of 20 mm for rheological measurements. The pure PEO and PCL were also solved and dried under the same condition to bring them the same history to those of the blends.

### Rheological measurements

Rheological measurements were carried out with a Stress Tech Fluids Rheometer using parallel plate geometry with diameter of 20 mm and the gap between the parallel plates being set as 0.35 mm. The rheological measurement was started after 3 min of thermal balance for each sample. All the samples were protected by  $N_2$  during the period of the experiments. Dynamic strain sweeps with a frequency of 6.28 rad/s were executed first for all the PEO/PCL blends and the homopolymers to

confirm their linear viscoelastic behaviors. Dynamic temperature sweeps were carried out at 6.28 rad/s with the strain amplitude controlled as 0.01 to detect the discontinuity of storage modulus dependent on decreasing temperature with a cooling rate of 1 °C/min. The first change of the slopes of storage modulus of the blends, dependent on decreasing temperature, were recognized as the cloud-point temperatures which were regarded as the starting points of phase separation in the blends. For all the temperature sweeps in this study, the gaps were temperature-compensated.

## Results and discussion

### Dynamic rheological properties of PEO and PCL

As known, the rheological property of an immiscible binary polymer blend is determined by the components, compositions, and phase structures of the blend. Rheology of a miscible binary polymer blend is always closely related to the interaction between different molecular chains of the components. Regardless of the miscibility, the rheological properties of the homopolymers play important roles in determining the rheological behaviors of the blends. Hereby, to understand the rheology of a binary polymer blend, for example, PEO/PCL, the rheological properties of the two homopolymers must be investigated beforehand.

Figure 1 shows the storage modulus ( $G'$ ), loss modulus ( $G''$ ), and complex modulus ( $G^*$ ) of PEO and PCL, dependent on strain amplitude ( $\gamma_0$ ) in dynamic strain sweeps with angular frequency of 6.28 rad/s at 70 °C. In general, the linear viscoelastic region of a sample can be recognized from the  $G'-\gamma_0$  plot. A critical value  $\gamma_{0,c}$  can be determined, when nonlinear behavior appears. The range of  $\gamma_0$  below  $\gamma_{0,c}$  is the linear viscoelastic region. From Fig. 1, it can be seen that strain-thinning effect appears for PEO when  $\gamma_0 > 0.62$ . This is reasonable because the molecular weight of PEO material used in this study is larger than its entanglement molecular weight of 2,160 g/mol reported by Niedzwiedz et al. [30] and Fetters et al. [31]. The disentanglement and orientation of PEO chains along the flow direction result in the strain-thinning phenomenon. While for PCL, a slight strain hardening appeared when  $\gamma_0$  increased from 0.13 to 0.50, which can be observed obviously from  $G'$  variations of PCL melt. In Fig. 1, a slight increase of  $G''$  of PCL melt with increasing  $\gamma_0$  can also be found within the experimental window, which is much later than that of  $G'$  and the amplitude is much smaller as well. As reported by Izuka et al. [32], the entanglement molecular weight of PCL is about 14,000 g/mol. The strain-hardening phenomenon of PCL used here can be interpreted by a network formation of the entangled PCL molecular chains, which is difficult to disentangle mainly because of the rigidity of the molecular main chains and the interactions between molecules under the experimental conditions. The strain-thinning behavior of PEO and the strain-hardening behavior of PCL show the nonlinear behavior of the polymer melts at  $\gamma_0$  values beyond the linear viscoelastic region at 70 °C. The nonlinear behavior of PEO and PCL melts are closely related to their melt structure variations on molecular level due to the too large strain amplitudes they suffered.

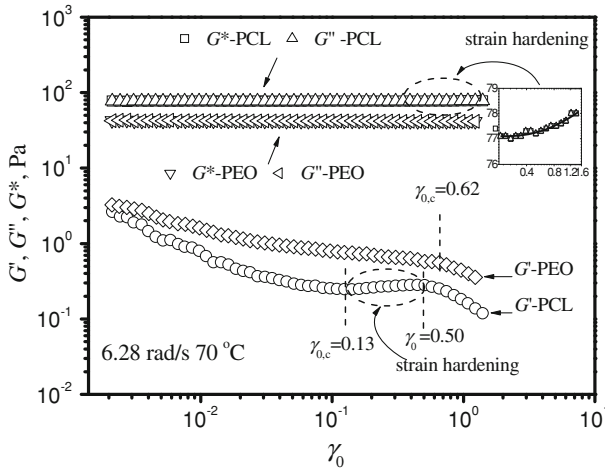


**Fig. 1**  $G'$ ,  $G''$ , and  $G^*$  dependent on  $\gamma_0$  of PEO and PCL

For PEO and PCL, the  $\sigma_0$ - $\gamma_0$  and  $(\sigma_0/\gamma_0)$ - $\gamma_0$  plots are shown in Fig. 2a, b. In Fig. 2a, both for PEO and PCL, the  $\sigma_0$  values are found to be linear to  $\gamma_0$ . In Fig. 2b, the  $(\sigma_0/\gamma_0)$  value of PEO is constant within the experimental range and the  $(\sigma_0/\gamma_0)$  value of PCL showed a very slight increase at  $\gamma = 0.67$ . Thus, from Fig. 2a, b, it seemed that PEO and PCL showed wider linear viscoelastic regions than those determined from  $G'$ - $\gamma_0$  plots in Fig. 1. While as it is known that the linear viscoelastic property of a polymeric fluid is closely related to its structure, its linear viscoelastic region should be decided by the stability of the fluid structure instead of any specific experimental method. The wider linear viscoelastic regions revealed from the  $\sigma_0$ - $\gamma_0$  and  $(\sigma_0/\gamma_0)$ - $\gamma_0$  plots than that from the  $G'$ - $\gamma_0$  plots may be due to the lower sensitivity of  $\sigma_0$  and  $\sigma_0/\gamma_0$  to the structure than that of  $G'$  of the materials. In fact, it can be seen from Fig. 1 that, for both PEO and PCL melts, the  $G'$  values are much smaller than the corresponding  $G''$  values, showing the weakness of the melts with very low  $G'$ . For such polymeric fluids, the structural variations which can be detected by the obvious changes of  $G'$  might not be detectable by the changes of the  $\sigma_0$ - $\gamma_0$  and  $(\sigma_0/\gamma_0)$ - $\gamma_0$  plots. Thus, in this study, the  $\gamma_{0,c}$  values of PEO and PCL were determined as  $\gamma_{0,c}(\text{PEO}) = 0.62$  and  $\gamma_{0,c}(\text{PCL}) = 0.13$  according to  $G'$ - $\gamma_0$  plots in Fig. 1, respectively.

Furthermore, when  $\gamma_0$  is much smaller than  $\gamma_{0,c}$ , both PEO and PCL show decreasing  $G'$  with increasing  $\gamma_0$ , which may be due to the hydrogen bonding in the melt bulk of PEO and PCL at 70 °C.

Within the linear viscoelastic regions,  $\gamma_0 = 0.01$  was selected for temperature sweeps of PEO and PCL at a dynamic angular frequency of 6.28 rad/s. The temperature-dependent  $G'$  of PEO and PCL are shown in Fig. 3a. The  $G'$  value of PCL almost keeps constant with the temperature decreasing from 160 to 70 °C. The  $G'$  value of PEO shows an obvious decrease with temperature decreasing from 160 to 130 °C, and then turns to be stable when temperature decreasing further from 130 to 70 °C. In Fig. 3b, c,  $G''$  and phase angle of PCL were all monotonic decreasing

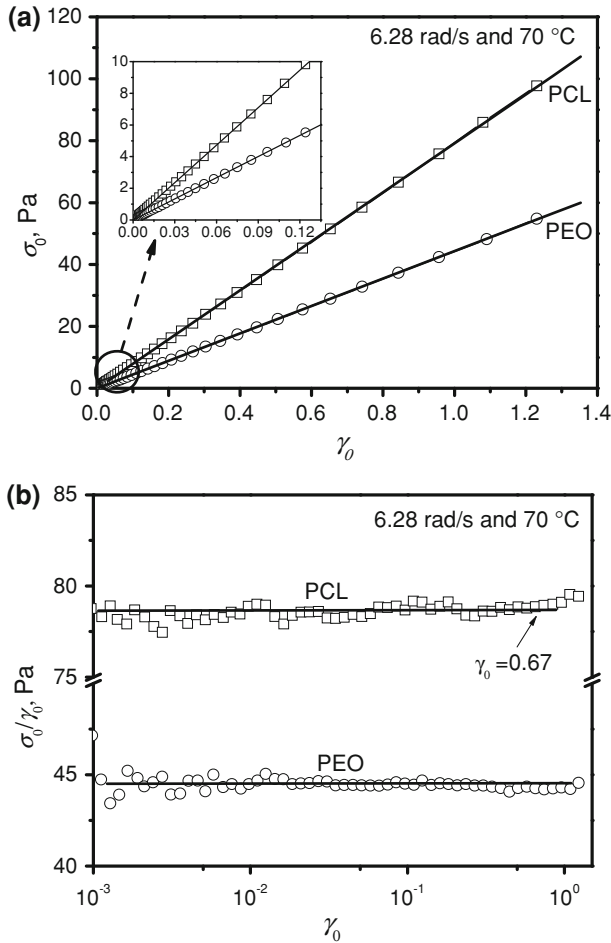


**Fig. 2** Relations between  $\sigma_0$  and  $\gamma_0$  in forms of **a**  $\sigma_0$ - $\gamma_0$  and **b**  $(\sigma_0/\gamma_0)$ - $\gamma_0$  for PEO and PCL in dynamic strain sweeps at 6.28 rad/s and 70 °C

functions of temperature, while  $G''$  and phase angle ( $\delta$ ) of PEO showed transition behaviors at 130 °C similar to that of  $G'$  of PEO. This observable abnormal rheological characteristic of PEO melt at temperatures higher than 130 °C can be attributed to its thermal stability [19]. In order to examine whether there is observable chain degradation of PEO, dynamic time sweeps at two temperatures of 120 and 160 °C were executed, respectively, for PEO melt at 6.28 rad/s with strain amplitudes controlled as 0.01. As shown in Fig. 4, the obtained complex viscosity of PEO remained almost constant at both 120 and 160 °C. This implied that no thermal degradation of PEO chains could be observed in the time sweep experiments. Thus, it can be concluded that no observable thermal degradation of PEO occurred in the dynamic temperature sweeps in Fig. 3. The abnormal

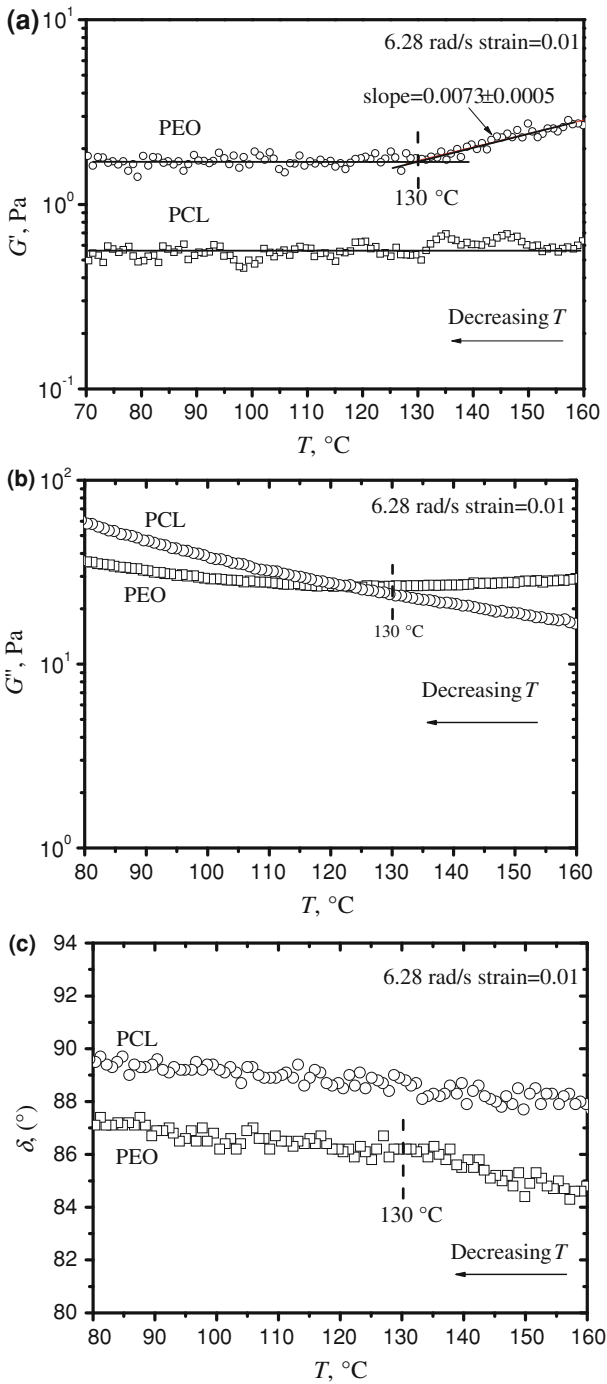


**Fig. 3** Dependence on decreasing temperature of **a**  $G'$ , **b**  $G''$ , and **c** phase angle ( $\delta$ ) of PEO and PCL melts at 6.28 rad/s with  $\gamma_0 = 0.01$



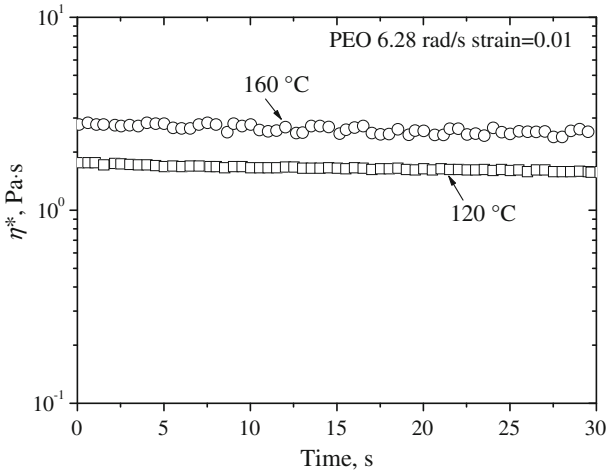


**Fig. 4** Dynamic time sweeps of PEO melt at 120 and 160 °C with strain amplitudes controlled as 0.01 and angular frequencies of 6.28 rad/s

rheological characteristics of PEO at temperatures higher than 130 °C may be due to the interactions between PEO molecular chains dependent on temperature.

For most thermoplastic polymeric materials, a decrease in temperature allows less thermal motion of macromolecular chains and smaller free volume in the polymeric fluids, which leads to an increase in intermolecular or intramolecular resistances thus, generally increased  $G'$  and  $G''$ . In Fig. 3a, b,  $G'$  of PEO and PCL seemed to be almost constant but  $G''$  of PEO and PCL increased with temperature decreasing from 130 to 70 °C for PEO and from 160 to 130 °C for PCL. It revealed that the influence of temperature on thermal mobility of macromolecular chains or free volume in PEO or PCL melts might be different from those in general polymeric materials. From this viewpoint, the modulus dependence on temperature of the investigated PEO and PCL melts in such a complex manner might be attributed to the hydrogen bonds in the fluids. And this might influence the determination of phase-separation temperature of a PEO/PCL blend by dynamic shear rheology. Investigations on phase separation of such polymer blends have not been reported yet.

#### Dynamic rheological properties of PEO/PCL blends

The dynamic strain sweep curves of PEO/PCL blends with the selected weight proportions of 80/20, 60/40, 50/50, 40/60, and 20/80 at 70 °C and 6.28 rad/s are shown in Fig. 5. According to the results of PCM [10] and TRSALS [11] observations, the PEO/PCL blends at 70 °C should behave as immiscible binary polymer blends. In general, in such immiscible binary polymer blends, the elasticity of the minor phase droplets result in larger  $G'$  of the blends than those of the two components at terminal frequencies [5–8]. This is true for the PEO/PCL blends at 70 °C. Within the whole experimental range of  $\gamma_0$ , PEO/PCL blends showed larger

$G'$  than those of the homopolymers. The compositional dependence of  $G'$  of the blends is shown in Fig. 6 as a slight “M”-shaped curve, with the  $G'$  data selected at  $\gamma_0 = 0.01$  from Fig. 5. The PEO/PCL blends at 70 °C showed positive deviations from the log-linear additivity rule, which is usually found in immiscible binary polymer blends mainly due to separated phase structures under weak enough shear conditions [33].

From Fig. 5, it can be noticed that all the PEO/PCL blends with different compositions in weight ratios showed no strain-hardening behaviors as that of PCL melt within the  $\gamma_0$  range from 0.13 to 0.50. The formation mechanism of strain-hardening behavior of PCL melt seemed to have been destroyed by the PEO component in the blends. Though PCL is believed to be immiscible with PEO at 70 °C, a small amount of PEO chains may still be dissolved in PCL phase and make the thermal mobility of PCL chains increased. This resulted in faster relaxation of the PCL molecular chains in the blends than in pure PCL melt. Thus, in the PEO/PCL blends, the strain-hardening behavior disappeared. This is understandable because the ether groups in PEO melt can rotate much more easily than the ester groups in PCL melt. Compared with PEO molecular chains, PCL molecular chains seem to be more rigid. Intercalation of small amount of PEO molecular chains can efficiently decrease the friction between two PCL molecular chains and make it easy for them to be released due to disentanglements, which might be closely related to the formation of the strain-hardening behavior of PCL melt in Fig. 1 and its disappearances in PEO/PCL blends in Fig. 5.

Furthermore, it can be noticed that almost all the curves of PEO/PCL blends in Fig. 5 can be divided into three parts by two typical values of  $\gamma_{0,1}$  and  $\gamma_{0,2}$ . When  $\gamma_0$  is smaller than  $\gamma_{0,1}$ , the  $G'$  values of all the PEO/PCL blends showed less dependence on  $\gamma_0$ , especially when PCL is the matrix. This may be due to the formation of the separated phase structures in the blends or due to the variations of

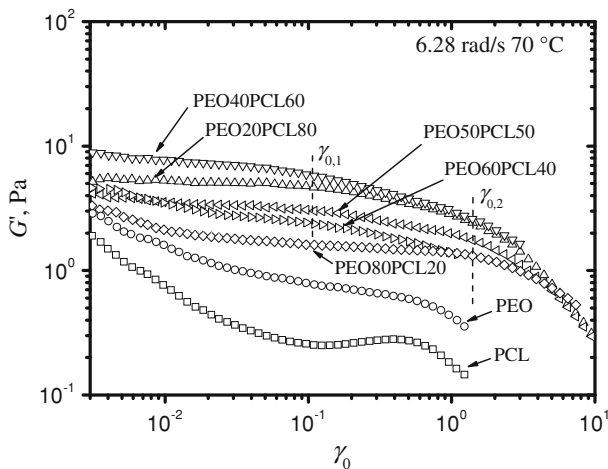


**Fig. 5** Dynamic strain amplitude dependence of  $G'$  of PEO, PCL, and their blends with different weight proportions at 6.28 rad/s and 70 °C

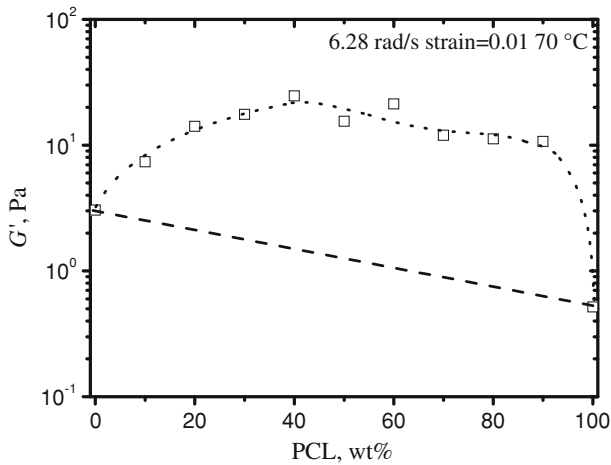


**Fig. 6** Dependence of  $G'$  of PEO/PCL blends on weight proportions at 70 °C and 6.28 rad/s with  $\gamma_0 = 0.01$ , all data points are selected from dynamic strain sweeps of the blends

the interactions between the molecular chains of both PEO and PCL phases according to small amounts of another component solved in. The difference of the  $G'$  dependent on  $\gamma_0$  of the blends with PEO as minor phase from those of the blends with PCL as minor phase at small  $\gamma_0$  showed that the influence of PEO on PCL is different from that of PCL on PEO based on the different molecular structures of the two components. For example, in Fig. 5, PEO80PCL 20 blend showed more obvious dependence of  $G'$  on  $\gamma_0$  while  $\gamma_0$  is smaller than about 0.01. When  $\gamma_0$  is larger than  $\gamma_{0,1}$  or  $\gamma_{0,2}$ , almost all the immiscible PEO/PCL blends with different weight ratios at 70 °C showed noticeable decreasing trends of the storage modulus. These two decreasing process of  $G'$  of the PEO/PCL blends can be attributed to the nonlinear viscoelastic responses of the two single phases in the melts of the blends.

Figures 7 and 8 showed the  $G'$  of PEO90PCL10 and PEO80PCL20 dependent on decreasing temperature. In Fig. 7, PEO90PCL10 showed a very slight decrease of  $G'$  with temperature decreasing from 160 to 107.7 °C. In comparison with PEO, such a slight decrease of  $G'$  can be ignored since its corresponding slope much smaller than  $0.0073 \pm 0.0005$  for PEO within the temperature range from 160 to 130 °C in Fig. 3. In Fig. 8, PEO80PCL20 even showed a slight increase of  $G'$  with a negative slope while temperature decreasing from 160 to 110.9 °C. Such observable changes of the temperature dependence of  $G'$  of PEO90PCL10 and PEO80PCL20 at higher temperatures implied that the special rheological characteristics of the  $G'-T$  plot of PEO melt with temperature higher than 130 °C in Fig. 3 can be eliminated by blending PEO with PCL. This indicated that the behaviors of PEO molecular chains were influenced by PCL molecular chains in the blends of PEO90PCL10 and PEO80PCL20 at temperatures higher than 130 °C. Importantly, the transition temperatures of 107.7 and 110.9 °C for PEO90PCL10 and PEO80PCL20 are much smaller than 130 °C, the transition temperature of pure PEO. The special rheological characteristics of the  $G'-T$  plot of PEO melt in Fig. 3 had little influence on the rheological properties of the PEO/PCL blends at temperatures

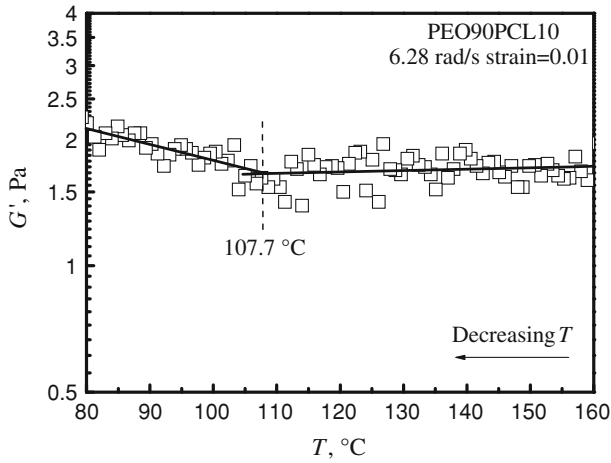


**Fig. 7** Dependence on temperature of  $G'$  of PEO90/PCL10 blend at 6.28 rad/s with  $\gamma_0 = 0.01$

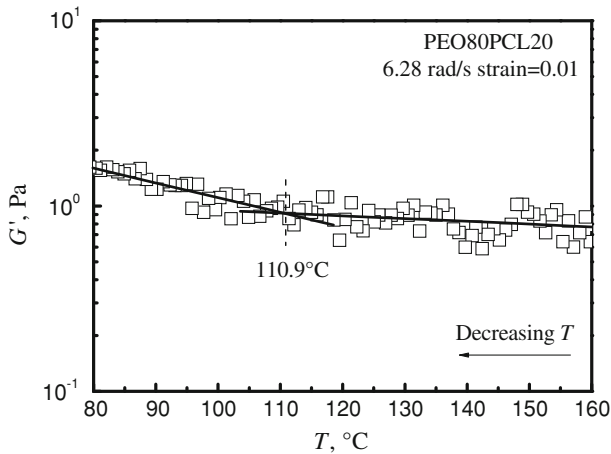


**Fig. 8** Dependence on temperature of  $G'$  of PEO80/PCL20 blend at 6.28 rad/s with  $\gamma_0 = 0.01$

higher than 130 °C. The  $G'$ – $T$  plots of PEO/PCL blends with weight proportions of 70/30, 60/40, 50/50, 40/60, 30/70, 20/80, and 10/90 were also checked carefully with temperature decreasing from 160 to 80 °C. In all these PEO/PCL blends, the influence of the abnormal rheological behavior of PEO component at temperature higher than 130 °C on the  $G'$ – $T$  plots was not observed.

#### Phase diagram and miscibility of PEO/PCL blends

As known, during the process of phase separation, the strength of the concentration fluctuations and the interfacial volume fraction determine the contribution of interfacial relaxation to the characteristic rheological behavior of the blend [34].

A concentration fluctuation generally appears in the homogeneous regime close to the phase-separation temperature in blend with critical composition, while off-critical composition does not exhibit observable concentration fluctuation [12, 15]. In a well phase-separated blend, an increase of  $G'$  value at low frequencies within the linear viscoelastic regime can usually be observed due to the effect of the interfacial tension between two phases of the blend.

For a phase-separating binary polymer blend system, both the contributions of the concentration fluctuations and the contributions of the interfacial tension may result in the  $G'$  increase and cause a discontinuity in its temperature dependence at low frequencies. Thus, the phase-separation process can be detected by identifying the discontinuity point in the  $G'-T$  plots. Such changes of the slopes of  $G'-T$  plots are often referred to as the binodal temperature of the blend, around which the turbidity always appears in the blend. Of course, at high frequencies,  $G'$  is little affected by the interfacial tension and thus, it is not sensitive to the phase-separation process in polymer blends. And it should be mentioned that the dynamic shear rheology is not always a suitable method to investigate the phase-separation process, comparing with other methods, such as SALS. The rheological properties of the blend in the phase-separated regime may vary quite complicatedly with blend composition due to the evolution of the phase structures, or be mainly controlled by the rheological properties of the two constituent components [14, 35], which may result in difficulty in determining the binodal temperatures of the blends by dynamic shear rheology. In addition, shear-induced phase separation (demixing) or shear-induced mixing might make the determination of the equilibrium phase-separation temperatures impossible.

From the results shown in Figs. 7 and 8, it can be seen that  $G'$  of PEO90PCL10 and PEO80PCL20 increased as soon as the temperature decreased below the transition temperatures of 107.7 and 110.9 °C for PEO90PCL10 and PEO80PCL20 blends, respectively. These characteristics of the blends were so different from the  $G'$  variations of PEO and PCL components at the same range of decreasing temperature shown in Fig. 3. The similar temperature-dependent storage modulus can be found for the PEO/PCL blends with other proportions, showing different transition temperatures which can be determined by the intersection of the two linearly fitted lines. The discontinuity of the  $G'-T$  plots for the PEO/PCL blends indicated that the structures of the blends at temperatures lower than the corresponding transition temperatures differ from those of the blends at temperatures higher than the transition temperatures. On the other hand, these results implied that the experimental conditions of 6.28 rad/s and a strain of 0.01 are suitable to make  $G'$  sensitive enough to detect the structural changes of the blends with decreasing temperature. Such increases of elasticity of the blends, compared with the constituent components, could be attributed to the occurrence of phase separation. Thus, the transition temperatures of the PEO/PCL blends, for example, 107.7 °C of PEO90PCL10 and 110.9 °C of PEO80PCL20, could be confirmed as the phase-separation temperatures determined by dynamic rheology at 6.28 rad/s with strain of 0.01. These transition temperatures of the PEO/PCL blends can be considered as the cloud-point temperatures similar to those in SALS method [11, 34].

Consequently, according to the dynamic temperature sweeps of the PEO/PCL blends, the phase diagram of the blends can be obtained and shown in Fig. 9, in

which the phase-separation temperatures of the blends determined by dynamic shear rheology are shown as  $T_{\text{Rheol}}$ . The  $T_{\text{b,TRSALS}}$  and  $T_{\text{s}}$  in Fig. 9 represent the binodal and the spinodal lines [11]. The binodal curve is drawn from the data of cloud-point temperatures measured by TRSALS method, whereas the spinodal curve is determined based on the linear Cahn–Hilliard theory.

The results showed that the PEO/PCL blends reveal a miscibility window of UCST character according to the dynamic rheology of the blends, which agrees with the results of Chuang et al. [11] by TRSALS. But there are obvious differences between the lines of  $T_{\text{Rheol}}$  and  $T_{\text{b,TRSALS}}$ . When the weight proportion of PCL is lower than about 60 wt%, the phase-separation temperatures of the PEO/PCL blends determined by dynamic shear rheology are much lower than the binodal line, indicating the well-known shear-induced mixing in the blends, though the molecular mass of the polymers in this article differed from those used by Chuang et al. [11]. For the PEO/PCL blends with more content of PCL, smaller values of  $T_{\text{Rheol}}$  than  $T_{\text{b,TRSALS}}$  appeared, and this indicated shear-induced phase separation or demixing occurred. Shear-induced mixing or demixing in the PEO/PCL blends revealed that the applied dynamic shear conditions influenced the phase-separation process; even small  $\gamma_0 = 0.01$  was selected within the linear viscoelastic regime at 6.28 rad/s.

Theoretically, low enough shear rates or frequencies do not induce any chain stretching [13] or any other changes of microstructures in the polymer blends. With dynamic shear rheology as a tool to detect the phase-separation process, the influence of the selected experimental shear condition is also expected to be weak enough not to induce mixing or demixing. But actually, this is difficult. To collect the response of a fluid to a dynamic shear flow is the basic viewpoints of dynamic rheology. The interaction between shear effect and phase-separation process cannot be avoided completely within the rheological experimental window, especially when high enough position resolution or good enough precision of torque

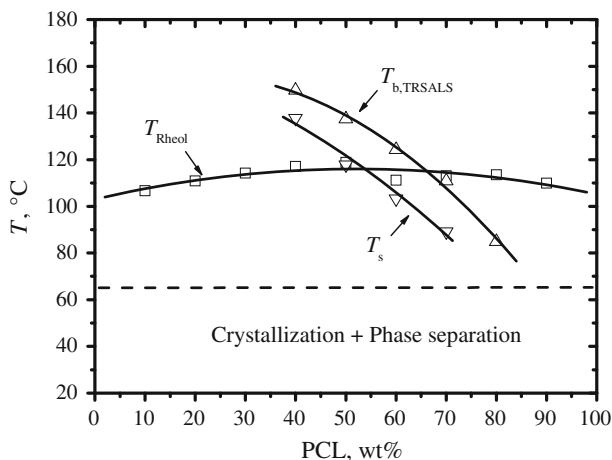


**Fig. 9** Phase diagram of PEO/PCL blends determined by dynamic rheology with the *dashed lines* plotted to guide eyes for  $T_{\text{m}}$  of the blends;  $T_{\text{b,TRSALS}}$  and  $T_{\text{s}}$  representing the binodal and spinodal temperatures according to reference [11]

measurement are required but not available for some polymer blends with very high or very low viscosities.

In the past decades, many researchers focused on the shear-induced effects on phase-separation process of polymer blends [16, 34]. For example, Zhang et al. [34] reported that the cloud-point temperatures of PzMSAN/PMMA blends cannot be affected by the applied oscillatory shear in the low frequency range, while the coagulation and growth of the blend morphology can be accelerated. Their further simulations based on the time-dependent Ginzburg–Landau (TDGL) equation qualitatively agree with their experimental findings. Jeon et al. [16] investigated the phase separation of polybutadiene (PB)/polyisoprene (PI) and found that the discontinuity of  $G'$  occurs at a frequency-dependent cloud-point temperature that extrapolates in the limit of zero frequency to the cloud point measured under quiescent conditions by optical microscopy. In general, a group of selected frequencies can be applied to obtain the corresponding cloud-point temperatures for polymer blends in which shear-induced mixing or demixing may occur. Then, the extrapolated cloud-point temperature can be regarded as the equilibrium phase-separation temperature. But in this study, the applications of very low angular frequency for PEO/PCL blends result in very small torque, which lies outside the experimental window of the apparatus. Further efforts are needed to investigate on the shear-induced mixing or demixing during phase-separation process in PEO/PCL blends.

According to the phase diagram in Fig. 9, for further discussion on the rheological characteristics of PEO/PCL blends in miscible and phase-separated region, the  $G'$  data of PEO/PCL blends at 160 and 70 °C were selected, respectively, from the dynamic temperature sweeps to obtain the compositional dependence of  $G'$ , as shown in Fig. 10. In general, it is common for binary miscible polymer blends to show linear additivity or log-linear additivity behaviors. In Fig. 10, the  $G'$  value of PEO at 160 °C is somehow larger than that of PEO90/PCL10 blend due to the special rheological characteristics of PEO at temperatures higher than 130 °C. If the  $G'$  value of PEO at 160 °C is extrapolated from the values below 130 °C, it is around that of PEO at 70 °C. Thus, obvious positive deviations from log-linear additivity mixing rules of  $G'$  of the blends at 160 °C can be observed. This proved that there are relatively strong interactions between PEO chains and PCL chains in miscible PEO/PCL blends, which destroys the special rheological characteristic of PEO phase in the blends. This also agrees with the other changes of the rheological properties of the PEO- or PCL-rich phase in the blends revealed by the macroscopic rheological properties of the blends, even though there may be only a small amount of PEO or PCL dissolved in the other polymer. When the temperature decreases from 160 to 70 °C, the  $G'$  of PEO/PCL blends show larger deviations from log-linear additivity mixing rules in phase-separated region than in miscible region at 160 °C. This increase of the positive deviations of the PEO/PCL blends can be attributed to the formation of phase-separated structures. Interestingly, if the temperature of PEO/PCL blend is increased directly from room temperature to 70 °C, the deviations of  $G'$  from log-linear additivity mixing rules are much larger than those of the phase-separated blends with temperature decreased from 160 °C. The PEO/PCL blends with temperature increased directly from room temperature

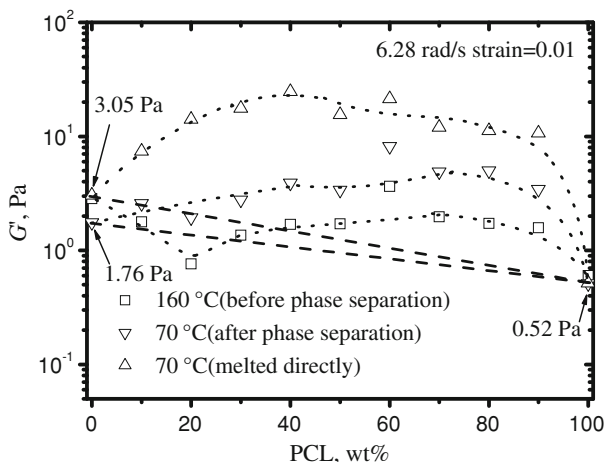


**Fig. 10** Compositional dependence of  $G'$  of PEO/PCL blends at 6.28 rad/s with  $\gamma_0 = 0.01$  at 160 °C (miscible) and 70 °C (phase separated), respectively, all data points are selected from dynamic temperature sweeps of the blends

are believed to be fully phase separated due to crystallization of PEO and PCL when solvent is evaporated from the solutions of the blends, which results in the larger deviations in Fig. 10. In addition, all the compositional-dependent curves of  $G'$  in Fig. 10 are of the same “M” shape of the curve with data selected from the dynamic strain sweeps in Fig. 6.

The slopes of  $G'-T$  plots of PEO/PCL blends in miscible regions at 6.28 rad/s with  $\gamma_0 = 0.01$  are found dependent on compositions of the blends with a “W” curve shape, and most of the data are negative, which are different from those of PEO and PCL components, shown in Fig. 11. A critical composition of 50/50 can be observed and this agrees with the  $T_{\text{Rheol}}$  line in Fig. 9. In miscible PEO/PCL blends with different compositions, the interactions between the PEO chains and PCL chains may be different due to the number ratio of the functional groups of the two components.

As known, frequency sweeps are always used to learn the dynamic rheological properties of binary polymer blends and their components. And on basis of frequency sweeps at a series of temperatures, time–temperature superposition (TTS) can be used to determine the phase-separated temperatures of the binary polymer blends. However, for the PEO/PCL blends in this study, their acceptable frequency sweep curves exceeded the measurement window of the instrument. In addition, the abnormal rheological behaviors of the components may make it difficult to determine phase-separation temperature of the PEO/PCL blends by TTS method.

It could be concluded that the results of dynamic shear rheology in this study showed that PEO/PCL is a blend with UCST character and there are interactions between the molecular chains of the two components due to hydrogen bonds in the blends, which agree with the DSC, PCM, and TRSALS investigations in references [9–11]. The criterion to confirm a miscible or immiscible blend by these experimental methods should be selected carefully.



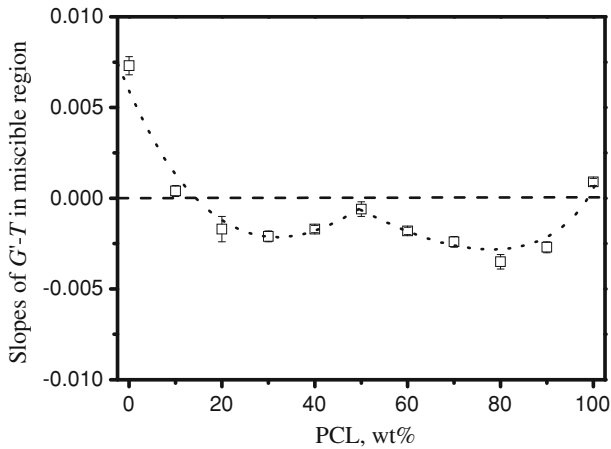


**Fig. 11** Compositional dependence of the slopes of  $G'-T$  plots of PEO/PCL blends in miscible regions at 6.28 rad/s with  $\gamma_0 = 0.01$

## Conclusions

By solution blending, PEO/PCL blends with different weight proportions were prepared and the phase diagram was established using rheometry. This rheologically determined phase diagram of PEO/PCL blends reveals a miscibility window of UCST character of the mixture. It should be mentioned that, though PEO showed abnormal temperature dependence of rheological properties at temperatures higher than 130 °C, it has little influence on the determination of miscibility and phase diagram of PEO/PCL blends. From the difference of the rheological properties of PEO/PCL blends from those of PEO, it is implied that there are molecular interactions between PEO and PCL components. In addition, when comparing the rheologically determined phase diagram with the results reported by Chuang et al. [11], one may find that shear-induced mixing or shear-induced phase separation might occur in phase diagram determination of the PEO/PCL blends using rheometry. Further rheological experiments are still needed to be executed with an instrument with a higher torque resolution for better investigation.

**Acknowledgments** The authors gratefully acknowledge the support of National Natural Science Foundation of China Programs (50903061, 50773082, 20974077, and 20804005).

## References

1. Jung JG, Bae YC (2010) Liquid–liquid equilibria of polymer solutions: Flory–Huggins with specific interaction. *J Polym Sci B* 48:162
2. Kim MH, Kim JH, Kim CK, Kang YS, Park HC, Won JO (1999) Control of phase separation behavior of PC/PMMA blends and their application to the gas separation membranes. *J Polym Sci B* 37:2950
3. Ermi BD, Karim A, Douglas JF (1998) Formation and dissolution of phase-separated structures in ultrathin blend films. *J Polym Sci B* 36:191

4. Orihara H, Nishimoto Y, Aida K, Na YH (2011) Three-dimensional observation of an immiscible polymer blend subjected to a step electric field under shear flow. *Phys Rev E* 83:026302
5. Gramespacher H, Meissner J (1992) Interfacial tension between polymer melts measured by shear oscillations of their blends. *J Rheol* 36:1127
6. Graebing D, Muller R, Palierne JF (1993) Linear viscoelastic behavior of some incompatible polymer blends in the melt. Interpretation of data with a model of emulsion of viscoelastic liquids. *Macromolecules* 26:320
7. Friedrich C, Gleinser W, Korat E, Maier D, Weese J (1995) Comparison of spheresize distributions obtained from rheology and transmission electron microscopy in PMMA/PS blends. *J Rheol* 39:1411
8. Li JQ, Ma GQ, Sheng J (2010) Linear viscoelastic characteristics of in situ compatibilized binary polymer blends with viscoelastic properties of components variable. *J Polym Sci B* 48:1349
9. Kuo SW, Lin CL, Chang FC (2002) Phase behavior and hydrogen bonding in ternary polymer blends of phenolic resin/poly(ethylene oxide)/poly( $\epsilon$ -caprolactone). *Macromolecules* 35:278
10. Qiu ZB, Ikehara T, Nishi T (2003) Miscibility and crystallization of poly(ethylene oxide) and poly( $\epsilon$ -caprolactone) blends. *Polymer* 44:3101
11. Chuang WT, Shih KS, Hong PD (2005) Kinetics of phase separation in poly( $\epsilon$ -caprolactone)/poly(ethylene glycol) blends. *J Polym Res* 12:197
12. Kapnistos M, Hinrichs A, Vlassopoulos D, Anastasiadis SH, Stammer A, Wolf BA (1996) Rheology of a lower critical solution temperature binary polymer blend in the homogeneous, phase-separated, and transitional regimes. *Macromolecules* 29:7155
13. Niu YH, Wang ZG (2006) Rheologically determined phase diagram and dynamically investigated phase separation kinetics of polyolefin blends. *Macromolecules* 39:4175
14. Kim JK, Son HW (1999) The rheological properties of polystyrene/poly(vinylmethylether) blend near the critical region and in the homogenous region. *Polymer* 40:6789
15. Kim JK, Lee HH, Son HW, Han CD (1998) Phase behavior and rheology of polystyrene/poly( $\alpha$ -methylstyrene) and polystyrene/poly(vinyl methyl ether) blend systems. *Macromolecules* 31:8566
16. Jeon HS, Nakatani AI, Han CC (2000) Melt rheology of lower critical solution temperature polybutadiene/polyisoprene blends. *Macromolecules* 33:9732
17. Song JY, Wang YY, Wan CC (1999) Review of gel-type polymer electrolytes for lithium-ion batteries. *J Power Sources* 77:183
18. Walls HJ, Zhou J, Yerian JA, Fedkiw PS, Khan SA, Stowe MK, Baker GL (2000) Fumed silica-based composite polymer electrolytes: synthesis, rheology, and electrochemistry. *J Power Sources* 89:156
19. Song YS (2006) Rheological characterization of carbon nanotubes/poly(ethylene oxide) composites. *Rheol Acta* 46:231
20. Wilson JS, Frampton MJ, Michels JJ, Sardone L, Marletta G, Friend RH, Samori P, Anderson HL, Cacialli F (2005) Supramolecular complexes of conjugated polyelectrolytes with poly(ethylene oxide): multifunctional luminescent semiconductors exhibiting electronic and ionic transport. *Adv Mater* 17:2659
21. Maitra A, Heuer A (2007) Cation transport in polymer electrolytes: a microscopic approach. *Phys Rev Lett* 98:227802
22. Chiu CY, Hsu WH, Yen YJ, Kuo SW, Chang FC (2005) Miscibility behavior and interaction mechanism of polymer electrolytes comprising LiClO<sub>4</sub> and MPEG-*block*-PCL copolymers. *Macromolecules* 38:6640
23. Lyons JG, Blackie P, Higginbotham CL (2008) The significance of variation in extrusion speeds and temperatures on a PEO/PCL blend based matrix for oral drug delivery. *Int J Pharm* 351:201
24. Lin WJ, Flanagan DR, Linhardt RJ (1999) A novel fabrication of poly( $\epsilon$ -caprolactone) microspheres from blends of poly( $\epsilon$ -caprolactone) and poly(ethylene glycol)s. *Polymer* 40:1731
25. Park SJ, Kim KS, Kim SH (2005) Effect of poly(ethylene oxide) on the release behaviors of poly( $\epsilon$ -caprolactone) microcapsules containing erythromycin. *Colloids Surf B* 43:238
26. Verreck G, Chun I, Li Y, Kataria R, Zhang Q, Rosenblatt J, Decorte A, Heymans K, Adriaensen J, Bruining M, Remoortere M, Borghys H, Meert T, Peeters J, Brewster M (2005) Preparation and physicochemical characterization of biodegradable nerve guides containing the nerve growth agent sabeluzole. *Biomaterials* 26:1307
27. Washburn NR, Simon CG Jr, Tona A, Elgendy HM, Karim A, Amis EJ (2002) Co-extrusion of biocompatible polymers for scaffolds with co-continuous morphology. *J Biomed Mater Res* 60:20
28. Lin CL, Chen WC, Kuo SW, Chang FC (2006) Sequence distribution affect the phase behavior and hydrogen bonding strength in blends of poly(vinylphenol-co-methyl methacrylate) with poly(ethylene oxide). *Polymer* 47:3436

29. Chiu CY, Chen HW, Kuo SW, Huang CF, Chang FC (2004) Investigating the effect of miscibility on the ionic conductivity of LiClO<sub>4</sub>/PEO/PCL ternary blends. *Macromolecules* 37:8424
30. Niedzwiedz K, Wischniewski A, Pyckhout-Hintzen W, Allgaier J, Richter D, Faraone A (2008) Chain dynamics and viscoelastic properties of poly(ethylene oxide). *Macromolecules* 41:4866
31. Fetters LJ, Lohse DJ, Milner ST, Graessley WW (1999) Packing length influence in linear polymer melts on the entanglement, critical, and reptation molecular weights. *Macromolecules* 32:6847
32. Izuka A, Winter HH, Hashimoto T (1992) Molecular weight dependence of viscoelasticity of polycaprolactone critical gels. *Macromolecules* 25:2422
33. Galloway JA, Macosko CW (2004) Comparison of methods for the detection of cocontinuity in poly(ethylene oxide)/polystyrene blends. *Polym Eng Sci* 44:714
34. Zhang ZL, Zhang HD, Yang YL, Vinckier I, Laun HM (2001) Rheology and morphology of phase-separating polymer blends. *Macromolecules* 34:1416
35. Kedrowski C, Bates FS, Wittzius P (1993) Dynamic scaling in spinodally decomposing isotopic polymer mixtures. *Macromolecules* 26:3448